Chapter 5

Addendum

The present study utilized mammalian HEK293 cells as a model expression system for screening mutational effects of the GluCl receptor. As discussed in Chapter 3, much cell-to-cell variability was observed during electrophysiology experiments on L9' mutants. Additional functional assays performed for silencing tool optimization, supplemental to those presented in Chapter 4, also displayed a great deal of variability and are the subject of this addendum.

Prior to introducing the monomeric YFP mutation, negative effects on IVM sensitivity imparted by the fluorescent protein insertion in the α subunit were first investigated by simple extraction of the YFP tag. Removal of YFP from the α subunit of (α)L9'F, (β)Y182F, and (β)RSR_AAA mutant receptors yielded ambiguous results (Figure 5-1A, B, C). Individually, the removal of YFP from α increased the high sensitivity component of the (α)L9'F mutant but eliminated the high sensitivity component from the (β)RSR_AAA mutant, while the (β)Y182F mutant remained unchanged. Assorted combinations of these mutations were equally puzzling (Figure 5-1D).

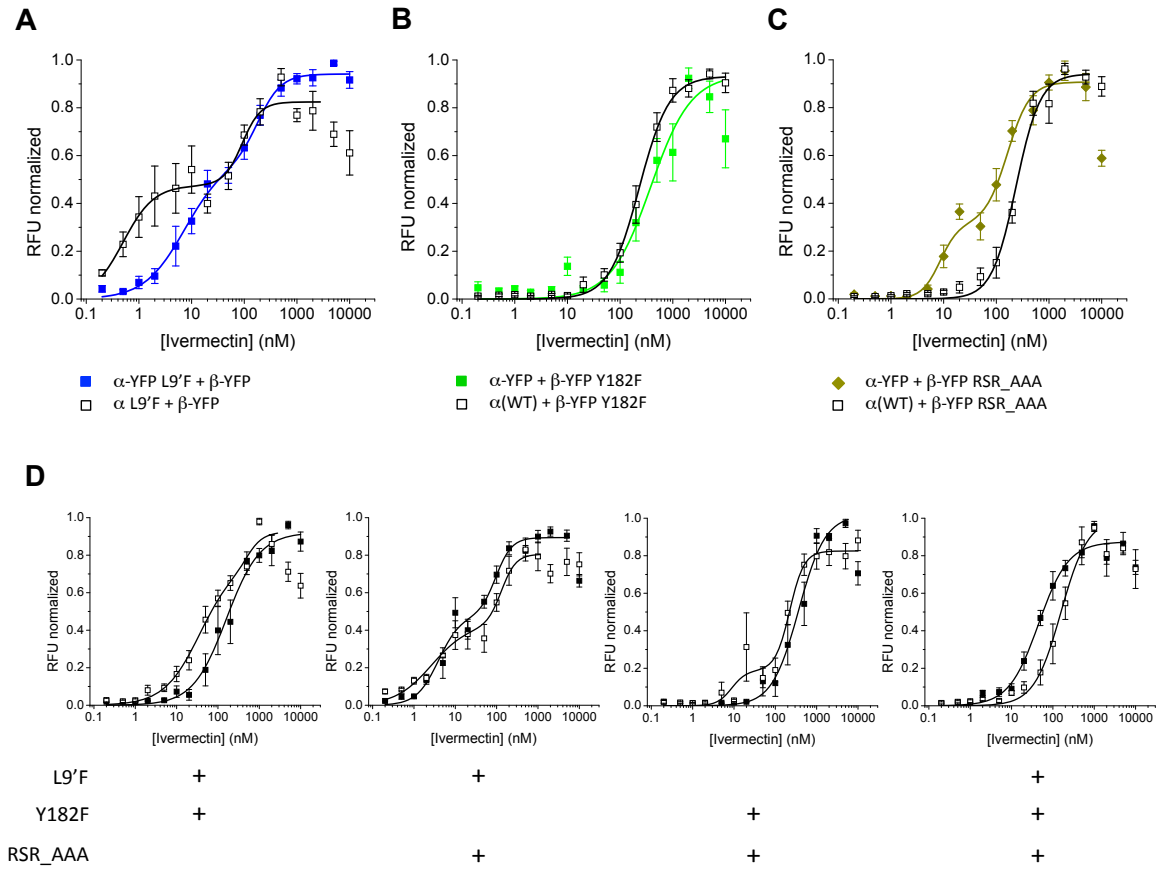

Figure 5-1. Removal of YFP from the α subunit affects IVM sensitivity. IVM activation was assayed using the FlexStation. Normalized IVM concentration-response curves showing removal of the YFP tag from the α subunit increased the high sensitivity component of the (α)L9'F mutant (*panel A.*) but eliminated the high sensitivity component from the (β)RSR_AAA mutant (*panel C.*) while IVM sensitivity of the (β)Y182F mutant (*panel B.*) was unchanged. *D.* Normalized IVM concentration-response curves of assorted mutant combinations with (filled symbol) and without (open symbol) YFP on the α subunit did not reveal a consistent effect.

In retrospect, oligomerization of the fluorescent fusion proteins presumably affected receptor stoichiometry in these experiments. The contradicting effects on the biphasic response of (α)L9'F and (β)RSR_AAA receptors, are in accordance with the proposed mutational implications. For example, in the ER, YFP oligomerization of α-α dimers, α-β dimers and β-β dimers presumably occur with the same prevalence. Removal

of YFP from the α subunit may boost its availability for the preferred α-β dimerization effect of the (α)L9'F mutation. This inadvertently reduces α-α dimerization while further promoting β subunit incorporation, visible by the enhanced high sensitivity component of the IVM concentration-response curve. The (β)RSR_AAA mutation, on the other hand, probably prevents β subunit degradation, but it does not have the heterodimer promotional effect of (α)L9'F. Because YFP tags of the β subunit were left intact, β-β dimers likely predominate, thereby sequestering the β subunit, resulting in primarily α homomer expression and a monophasic response.

The biphasic IVM response of (α)L9'F mutant receptors (with YFP removed from α) exhibited the largest high sensitivity component observed at the time. The IVM-induced currents associated with the two components of this mutant were examined by electrophysiology and compared to WT and (β)Y182F receptors (also with YFP removed from α). Whole-cell currents were recorded from transfected HEK293 cells in voltage-clamp with bath perfusion of 1, 5, and 50 nM IVM. The kinetic response was highly variable, yet two modes of activation were observed: a "slow" mode requiring minutes to peak current with some evidence of recovery (Figure 5-2A, black lines) and a "slower" mode which did not peak within the 5-minute application of IVM, rather, it continued to increase even upon removal of IVM from the bath (Figure 5-2A, red lines). The current magnitude of "slower" mode responses often resembled the steady-state current of the "slow" mode response. Nevertheless, pooled data still indicate a significant increase in mean peak current for the (α)L9'F mutant at 1 nM IVM (Figure 5-2B) and normalization of the mean response reveals a significant increase in IVM sensitivity at both 1 and 5 nM IVM for (α)L9'F (Figure 5-2C). Interestingly, no "slower" responses were observed for

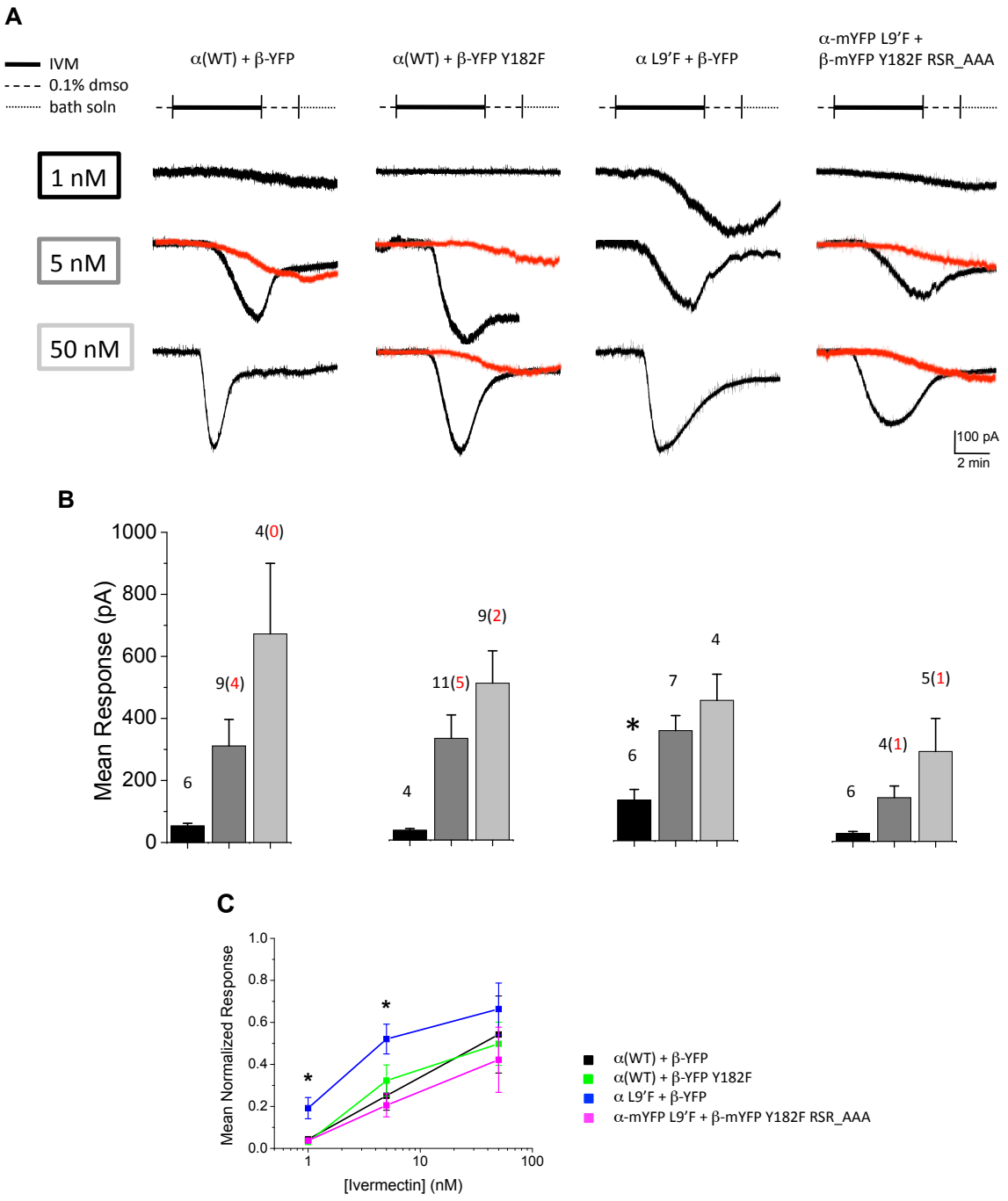

Figure 5-2. Electrophysiology with IVM. *A*. Whole-cell IVM-induced currents recorded from HEK293 cells in voltage-clamp. IVM concentrations of 1, 5, and 50 nM were applied for 5 minutes by bath perfusion. Two modes of activation were observed: 'slow' (*black traces*) and 'slower' (*red traces*). *B*. The (α)L9'F mutant shows a significant increase in mean peak current compared to WT at 1 nM IVM. The total number of cells recorded (*black numbers*) and the number of cells exhibiting 'slower' responses (*red numbers*) are indicated. *C*. Response normalization shows a significant increase in IVM sensitivity at both 1 and 5 nM IVM for (α)L9'F mutant.

the (α)L9'F mutant. At a much later date, similar recordings were obtained for the optimized receptor, α-mYFP L9'F + β-mYFP Y182F RSR_AAA. This receptor displayed both "slow" and "slower" type currents and did not appear to be significantly different from WT. These results were quite discouraging as they took place before neuronal silencing experiments.

The variability observed in the electrophysiological recordings of GluCl in HEK293 cells with IVM may be related to the high and low sensitivity responses observed in electrophysiological recordings with glutamate (Chapter 3), but it is difficult to speculate on the cause. Whether the "slower" IVM-induced currents contribute significantly to the population-based concentration-response curves obtained on the FlexStation seems unlikely as the magnitude of the response is minimal even after 5 minutes. It may be that "slower" currents are conducted by α homomers from cells that did not incorporate both α and β plasmid vectors during transfection. Since HEK293 cells were also cotransfected with soluble GFP to select cells for recording, cells that may have been expressing only the α subunit with no YFP tag would still have been included. Such variability caused by transfection, however, seems improbable since HEK293 cells are typically transfected with high efficiency. Nonetheless, recording from HEK293 cells intentionally transfected with only the α subunit would easily determine if "slower" currents are in fact conducted by α homomers.

Taking into account the slow activation kinetics of IVM and possible long-term accumulation of steady-state currents, mutants were incubated for 1 hour with varying concentrations of low IVM, and then assayed on the FlexStation using a single polarizing concentration of KCl to magnify the response. The EC_{50} concentration of 25 mM KCl

(Figure 5-3A, B) was used for the most sensitive detection of differential activation by low IVM and to avoid a saturating change in membrane potential. During the assay, addition of 25 mM KCl produced a negative signal (Figure 5-3C). This implies that long-term application of low IVM depolarizes cells to such an extent, that addition of an otherwise depolarizing amount of KCl induces repolarization of the membrane. The range of repolarization produced by a single dose of KCl reveals that long-term application of low IVM induces depolarization in concentration-dependent manner (Figure 5-3D). As expected, the (α)L9'F mutation increased sensitivity to IVM. Addition of the (β)Y182F mutation still reduced the (α)L9'F effect, but this double mutant maintained a significant increase in IVM sensitivity compared to the original tool used for silencing.

The A206K monomeric YFP mutation was essential toward the development of an optimized receptor. Even so, monomerization of YFP tags did not resolve the variability issues observed with GluCl in HEK293 cells. In the initial trial, the optimized GluCl α-mYFP L9'F + β-mYFP Y182F RSR_AAA receptor showed ~2 orders of magnitude greater sensitivity to IVM than the original tool used for silencing (Chapter 4, Figure 4-12). Both the optimized and original receptors were then assayed two additional times to ensure repeatability, and on average, the sensitivity improvement was maintained (Figure 5-4A). Examination of individual experiments, however, revealed the fraction of the high sensitivity component of the optimized receptor varied from day-to-day (Figure 5-4B).

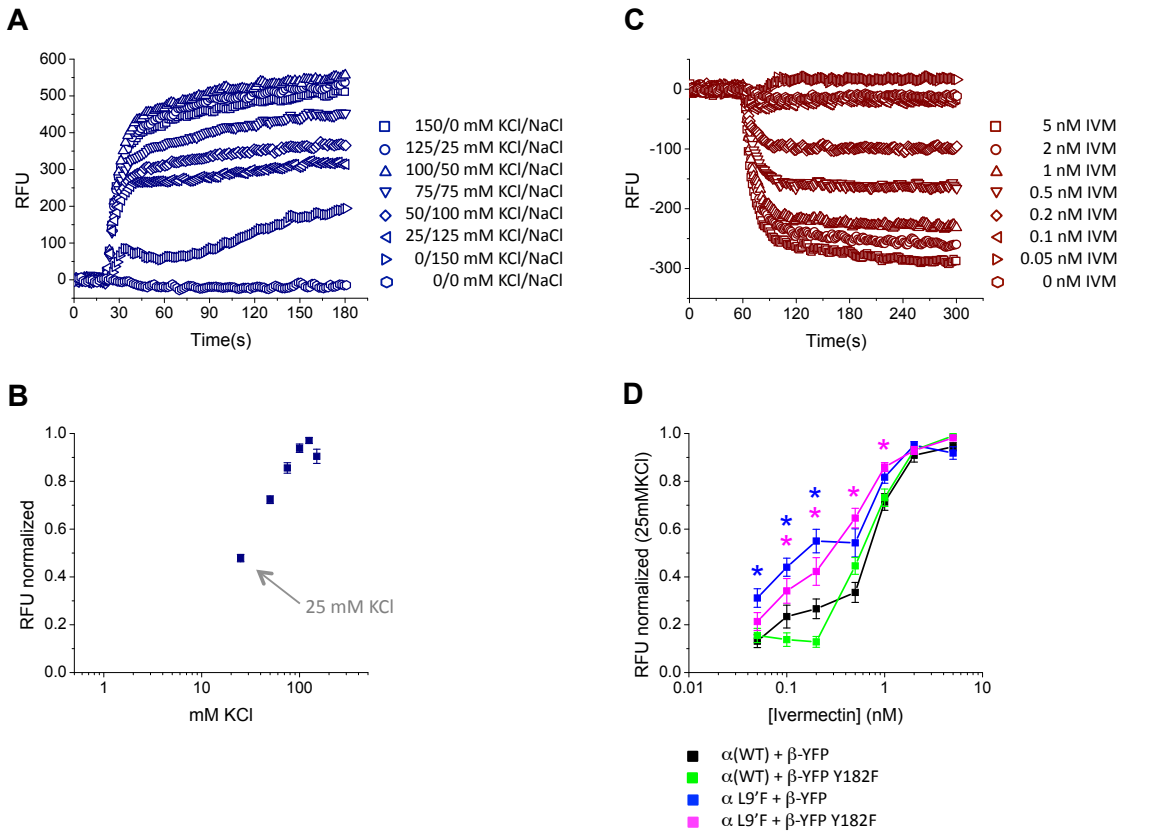

Figure 5-3. Preincubation with low IVM induces a concentration-dependent response. *A&B*. KCl-induced depolarization of nontransfected HEK293 cells reveals an EC_{50} of 25 mM. *C*. Transfected HEK293 cells were incubated for 1 hr with varying concentrations of low IVM, then assayed on the FlexStation with 25 mM KCl. Application of 25 mM KCl induced repolarizing (negative-going) signals in an IVM concentration-dependent manner. *D*. Response normalization reveals significantly increased IVM sensitivity for (α)L9'F and (α)L9'F+(β)Y182F mutant receptors compared to the original silencing tool, (**β**)Y182F.

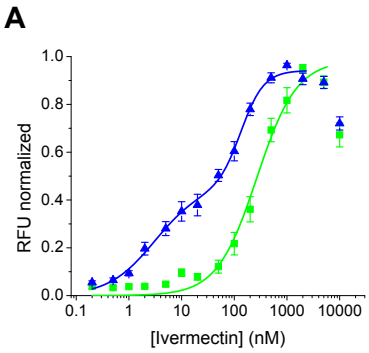

		1st comp	EC_{50} (μM)	Hill	EC_{50} (μM)	Hill	n
▲	α-mYFP L9'F + β-mYFP Y182F RSR_AAA	0.48	3.04 ± 1.41	1.00 ± 0.24	134.49 ± 21.03	2.01 ± 0.56	18
■	α-YFP+ β-YFP Y182F				267.32 ± 43.36	1.15 ± 0.15	18

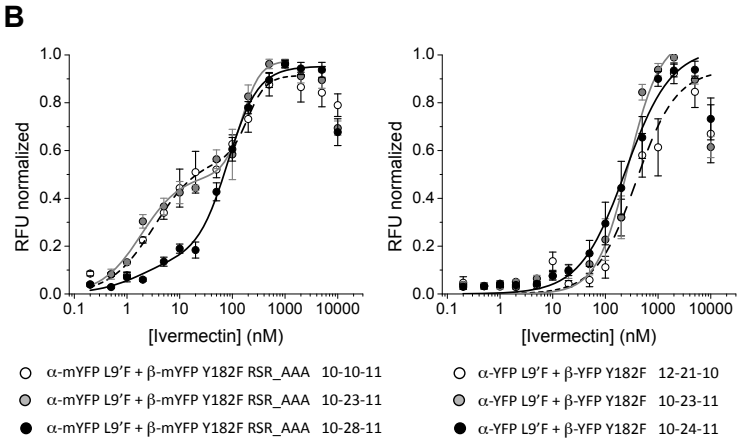

Figure 5-4. Functional assay repeatability of the optimized vs. original receptor silencing tools. IVM activation was assayed using the FlexStation. *A*. Optimized receptor maintains increased IVM sensitivity following triplicate measurements. Ivermectin activation parameters are presented in the corresponding table. *B*. Individual experiments reveal the high sensitivity component fraction of the optimized receptor varies from day-to-day. The consistent concentration-response of the original receptor ensures repeatability of the functional assay.

A host of additional experiments were subsequently performed in attempt to determine the source of this variability. Possible contributing factors tested included cell density, fresh culture media, fresh transfection reagent, the time posttransfection, and the passage number of the cells. All conditions produced a two-component curve with high sensitivity component fractions that varied remarkably (Figure 5-5A). Averaging all ten concentration-response curves of the optimized receptor still showed an improvement over the original silencing tool (Figure 5-5B, C). Time-dependent signal run-down was certainly a contributing factor, but it had been observed even with the WT receptor (Figure 5-6). Thus, the source of high IVM sensitivity variability remains to be determined.

Despite the many issues with variability, FlexStation assays of GluCl mutant receptors in HEK293 cells still served as a successful screening method for generating an optimized neuronal silencing tool. Though the original α-XFP + β-XFP Y182F receptor was effective in silencing neurons, the optimized α-mXFP L9'F + β-mXFP Y182F RSR_AAA receptor is significantly improved. Functional experimentation throughout the optimization process has provided a better understanding of structure-function relationships and subunit expression patterns of the GluCl receptor.

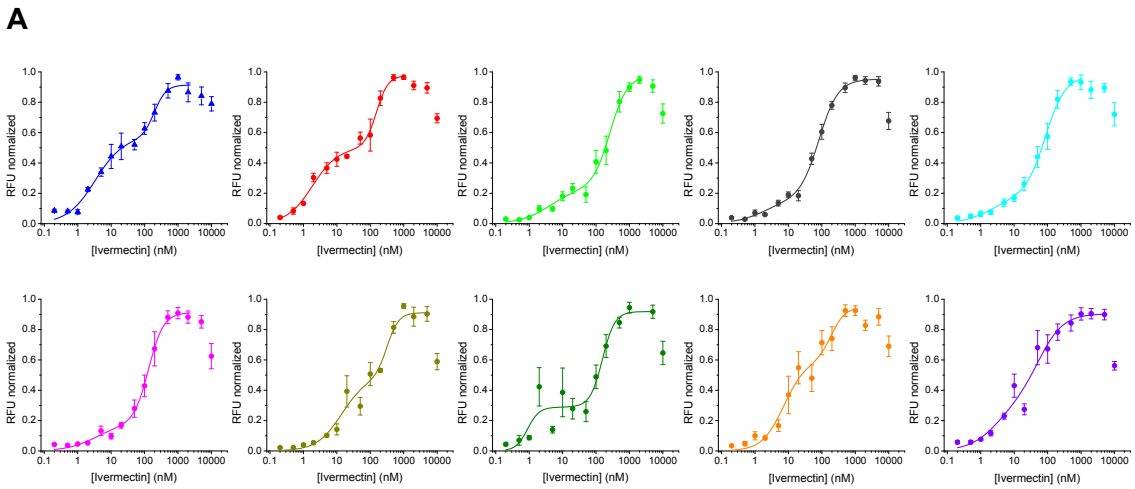

			1st comp	EC_{50} (μM)	Hill	EC_{50} (μM)	Hill	NOTES
●	α-mYFP L9′F + β-mYFP Y182F RSR_AAA	10-10-11 Plate2	0.37	3.35 ± 1.36	1.04 ± 0.27	196.26 ± 49.81	2.50 ± 1.64	P6 (N1)
●	α-mYFP L9′F + β-mYFP Y182F RSR_AAA	10-23-11 Plate1	0.51	1.88 ± 0.53	1.15 ± 0.28	153.28 ± 22.41	2.50 ± 0.86	P10 (N2)
●	α-mYFP L9′F + β-mYFP Y182F RSR_AAA	10-24-11 Plate2	0.24	4.17 ± 5.46	1.00 ± 0.68	260.68 ± 53.17	1.70 ± 0.55	P10 (N3)
●	α-mYFP L9′F + β-mYFP Y182F RSR_AAA	10-28-11 Plate1	0.17	1.92 ± 3.30	1.00 ± 0.86	82.33 ± 13.96	1.51 ± 0.28	P11 (N3)
●	α-mYFP L9′F + β-mYFP Y182F RSR_AAA	11-04-11 Plate1	0.18	2.06 ± 3.76	1.00 ± 0.85	86.37 ± 17.10	1.45 ± 0.37	P13; 18,000 cells/well
●	α-mYFP L9′F + β-mYFP Y182F RSR_AAA	11-04-11 Plate2	0.20	3.52 ± 4.93	1.00 ± 0.68	133.10 ± 16.40	1.96 ± 0.41	P13; 17,000 cells/well
●	α-mYFP L9′F + β-mYFP Y182F RSR_AAA	11-25-11 Plate1	0.53	13.98 ± 12.40	1.17 ± 0.64	317.79 ± 130.56	2.50 ± 1.79	P18; new media; new expressfect
●	α-mYFP L9′F + β-mYFP Y182F RSR_AAA	11-25-11 Plate2	0.31	0.89 ± 0.44	2.50 ± 2.81	155.28 ± 41.67	2.36 ± 1.36	P18; new media
●	α-mYFP L9′F + β-mYFP Y182F RSR_AAA	11-28-11 Plate1	0.63	7.26 ± 4.95	1.33 ± 0.63	191.35 ± 114.68	2.06 ± 2.82	P19; 24 hrs
●	α-mYFP L9′F + β-mYFP Y182F RSR_AAA	11-29-11 Plate1	0.37	3.09 ± 15.78	1.18 ± 1.28	55.98 ± 114.63	1.00 ± 1.52	P19; 48 hrs

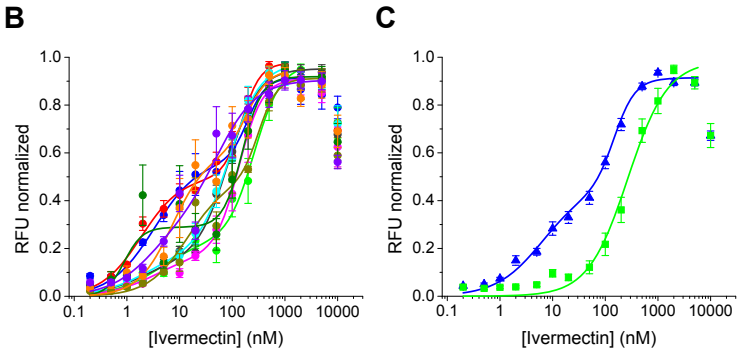

Figure 5-5. The high IVM sensitivity component of the optimized receptor is remarkably variable in HEK293 cells. IVM activation was assayed using the FlexStation. *A*. Additional assays of the optimized receptor considered the influence of cell density, fresh culture media, fresh transfection reagent, the time posttransfection, and the passage number of the cells. All conditions produced a two-component curve with varying fractions of high IVM sensitivity. Ivermectin activation parameters are presented in the corresponding table. The source of variability was not determined. *B&C*. Averaging all ten concentration-response curves of the optimized receptor still shows increased sensitivity compared to the original silencing tool.

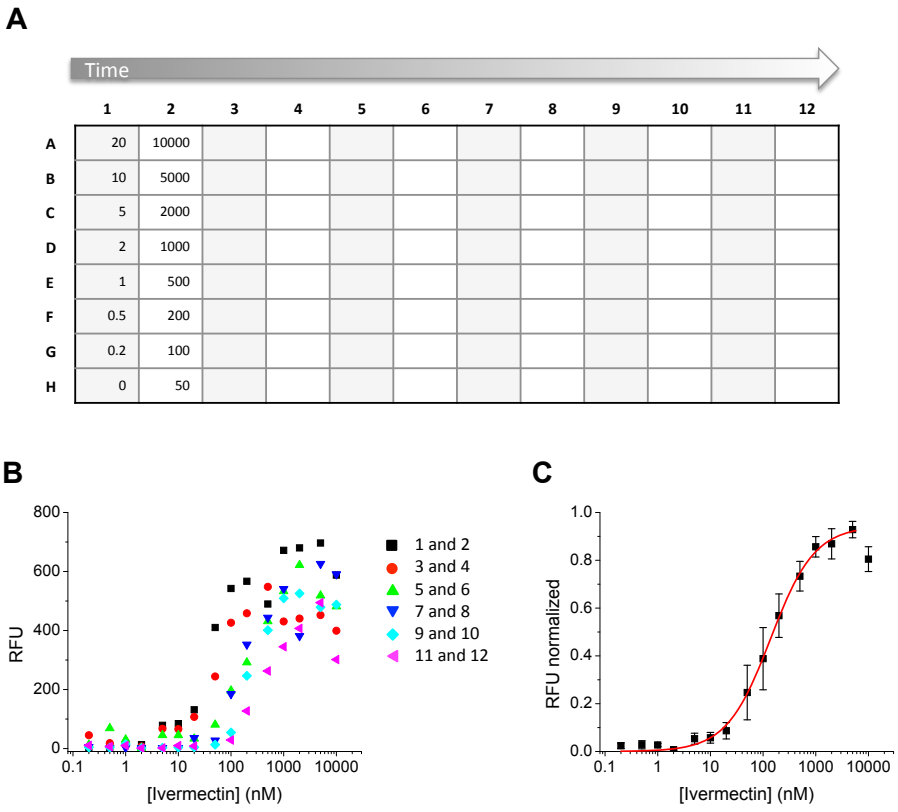

Figure 5-6. Time-dependent run-down of RFU signal. IVM activation was assayed using the FlexStation. *A*. FlexStation experimental design. Different concentrations of IVM are applied to each well. The IVM-induced signal of column 1 is detected for five minutes before moving on to column 2. The time lag between IVM application and signal detection remains constant. One 96-well plate assay takes one hour to complete. *B*. Two columns are combined for a single 15-point concentration response curve. Over time, from columns 1 and 2 (*black*) to columns 11 and 12 (*magenta*), raw signals are reduced in magnitude and concentration dependence is right-shifted. *C*. Despite signal run-down, an exemplary normalized concentration-response relationship is well fit to the Hill equation. Chi^2 per degrees of freedom = 0.00036. R^2 = 0.99772.

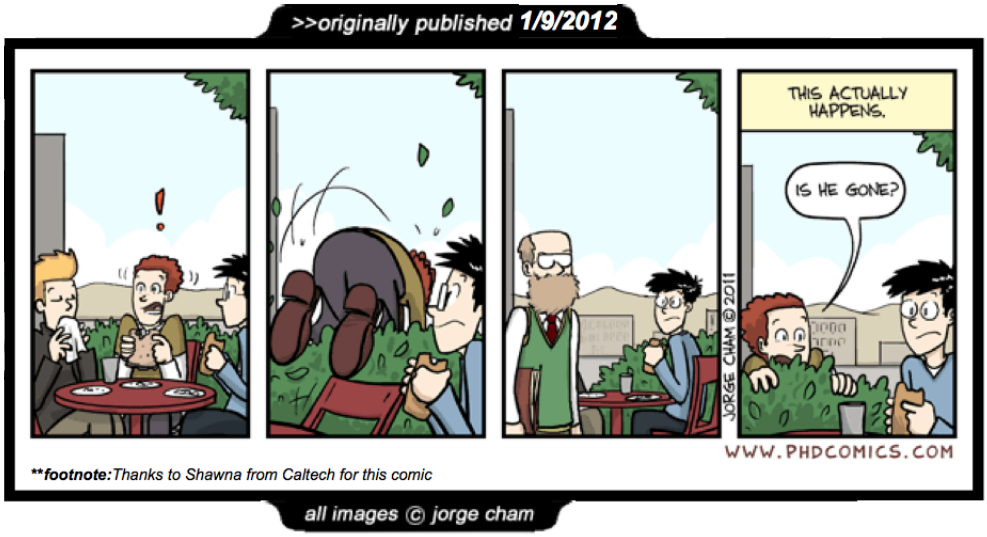
>>originally published 1/9/2012
!
THIS ACTUALLY HAPPENS.
IS HE GONE?
JORGE CHAM © 2011
WWW.PHDCOMICS.COM
**footnote: Thanks to Shawna from Caltech for this comic
all images © jorge cham